Research Article

Scattered light imaging beyond the memory effect using the dynamic properties of thick turbid media

Yuyang Shui[a] **Ting Wang,**[b] **Jianying Zhou,**[a,c] **Xin Luo,**[a] **Yikun Liu**[a,b,c,*] **and Haowen Liang**[a,c,*]

[a]Sun Yat-Sen University, State Key Laboratory of Optoelectronic Materials and Technologies, School of Physics, Guangzhou, China
[b]Sun Yat-Sen University, Guangdong Provincial Key Laboratory of Quantum Metrology and Sensing, School of Physics and Astronomy, Zhuhai, China
[c]Southern Marine Science and Engineering Guangdong Laboratory, Zhuhai, China

Abstract. Scattered light imaging through complex turbid media has significant applications in biomedical and optical research. For the past decade, various approaches have been proposed for rapidly reconstructing full-color, depth-extended images by introducing point spread functions (PSFs). However, because most of these methods consider memory effects (MEs), the PSFs have angular shift invariance over certain ranges of angles. This assumption is valid for only thin turbid media and hinders broader applications of these technologies in thick media. Furthermore, the time-variant characteristics of scattering media determine that the PSF acquisition and image reconstruction times must be less than the speckle decorrelation time, which is usually difficult to achieve. We demonstrate that image reconstruction methods can be applied to time-variant thick turbid media. Using the time-variant characteristics, the PSFs in dynamic turbid media within certain time intervals are recorded, and ergodic scattering regimes are achieved and combined as ensemble point spread functions (ePSFs). The ePSF traverses shift-invariant regions in the turbid media and retrieves objects beyond the ME. Furthermore, our theory and experimental results verify that our approach is applicable to thick turbid media with thickness of 1 cm at visible incident wavelengths.

Keywords: scattered light imaging; memory effect; thick turbid media; image reconstruction.

1 Introduction

Improving the quality of optical imaging is a primary goal in optical research. However, most objects and their surroundings, such as biological tissues and smog, are optically complex and turbid, inducing strong scattering light and drastically degrading image quality. Thus imaging through opaque diffusive media has become an important technical challenge, and many methods have been proposed to address this fundamental problem. Straightforward strategies that use only unscattered, "ballistic" photons selected by optical coherence tomography,[1] two-photon microscopy,[2] or holographic gating[3] have proven to be useful but not efficient because the number of ballistic photons that can be used is intrinsically limited. Wavefront shaping[4–8] through phase compensation with a spatial light modulator is an alternative solution that allows focusing and imaging through stronger scattering samples. Furthermore, a variety of improved approaches have been proposed with the initial assistance from guide stars[9,10] and known objects.[11,12] Matrix factorization combined with linear fluorescence has shown its capability to reconstruct the transmission matrices in biological microscopy.[13,14] The constructive two-photon interference formed by the thin dynamic scattering layer also enables direct imaging of the object.[15] With the development of machine learning, neural network-based imaging methods have demonstrated their ability to handle dynamic scattering and additional noise.[16,17]

A breakthrough approach that exploits inherent angular correlations in scattered speckle patterns[18–20] was used to successfully eliminate prior calibration with reference sources;

*Address all correspondence to Yikun Liu, liuyk6@mail.sysu.edu.cn; Haowen Liang, lianghw26@mail.sysu.edu.cn

however, the sequential scanning illumination is applicable only to stationary objects.[21] In addition, the intensity autocorrelation between the object image and the object can be reconstructed using a phase retrieval algorithm.[22–24] Optical imaging using the Fourier-domain shower-curtain effect has also yielded results in dynamic turbid media.[25] The core concept of these approaches is to consider the scattering medium as a "lens" so that the medium can be described by a point spread function (PSF). Based on this technique, high-speed, full-color images in scattering media can be reconstructed over large ranges.[26] Moreover, the PSF of a scattering medium can be extended to a depth that can be used for three-dimensional (3D) imaging.[27,28] The DiffuserCam, which uses a well-designed compress sensing algorithm, was proposed for 3D light-field imaging, and applies a single diffuser rather than a lens array.[29] Important results were also achieved using the noninvasive optical imaging by speckle ensemble technique,[30,31] demonstrating that the ensemble average of the PSF can be separated into a normal imaging part and a variance part for weak scatters, allowing targets to be reconstructed by microlens arrays or rotating scatters. However, the PSF is angular shift invariant over a very limited range of angles.[19,20] This phenomenon is known as the memory effect (ME). An increase in the thickness of the scattering medium leads to a limited expansion of the ME range, which hinders the use of these techniques in wider applications. Imaging through diffusers with larger ranges has attracted increasing attention, and many breakthroughs have been achieved through various algorithms and optical designs.[32–35] Therefore, the development of a general approach that is applicable to thick turbid media is essential for imaging scenarios that are currently inaccessible.

Based on the above description, we found that the PSF concept can be modified and extended for imaging through a thick turbid medium as long as the medium is time variant. Throughout the slowly changing scattering medium, a series of PSFs can be obtained and combined as an ensemble point spread function (ePSF) to achieve ergodicity.[36] The ePSF traverses the shift-invariant regions of the turbid medium and can retrieve objects beyond the ME range. In our experiment, we successfully applied this approach and reconstructed objects in a 1-cm-thick container filled with turbid liquid and dispersed calcium carbonate ($CaCO_3$) particles at visible incident wavelengths. The reconstruction range approaches that of a scattering system and is beyond the ME range. Compared with conventional single-exposure image recovery methods in static scattering media, the dynamic media allow a larger reconstruction range and a longer lifetime for the measured scattering properties. The dual advantages in time and space introduce the possibility of developing more applications in fields ranging from biology to medicine.

2 Principle

A PSF is an impulse response of a focused optical system. The intensity distribution of the light field under incoherent illumination is described by a convolution, $I = O * \text{PSF}$, where I and O are the intensity distributions on the image and object planes, respectively, and the symbol $*$ denotes the convolution operation. Several studies have proposed that thin turbid media can be considered lenses,[37,38] with the scattering properties determined by the PSF:

$$I(x_i, y_i) = \iint \text{PSF}(x_i, y_i; x_o, y_o) O(x_o, y_o) \mathrm{d}x_o \, \mathrm{d}y_o, \quad (1)$$

where (x, y) are the spatial coordinates and the subscripts i and o denote the image and object planes, respectively. In this case, I and the PSF are both complicated speckle patterns, and Eq. (1) is valid only within a shift-invariant region known as the ME range. By regarding the imaging system as a "black box," object O can be restored through a deconvolution process with the PSF measured by a reference point.

If the turbid property changes or the object O moves beyond the ME range, the PSF and image I must change simultaneously to ensure that Eq. (1) remains valid. For a time-variant scattering medium, Eq. (1) is valid only when the exposure time is shorter than the decorrelation time of the scattering patterns. If the exposure time is longer than the decorrelation time, the captured PSF and image I are the summation of different scattering states. Each scattering state describes a certain scattering channel for a group of incident photons. The concept of summing different scattering states is also applicable to multiple capturing applications. In these cases, Eq. (1) is rewritten as

$$\sum_n I_n(x_i, y_i) = \sum_n \iint \text{PSF}_n(x_i, y_i; x_o, y_o) O(x_o, y_o) \mathrm{d}x_o \, \mathrm{d}y_o, \quad (2)$$

where n is the serial number of each pair of I and PSF. As the time varying process is physically continuous, the summation notation in Eq. (2) can be moved inside the integral and rewritten as

$$\text{eI}(x_i, y_i) = \iint \text{ePSF}(x_i, y_i; x_o, y_o) O(x_o, y_o) \mathrm{d}x_o \, \mathrm{d}y_o, \quad (3)$$

where $\text{ePSF} = \sum_n \text{PSF}_n$ and $\text{eI} = \sum_n I_n$ are called the ePSF and ensemble image, respectively. In contrast to the normal PSF, the ePSF is superposed by each PSF_n that traverses different shift-invariant regions in the turbid medium.

Thus the ePSF describes almost all the scattering properties and optical information of the medium for the closed scattering system, which contains finite ergodic states, resulting such that the objects can be retrieved outside the ME range of any single scattering state. Higher summation times yield more complete ensemble scattering states that can be recorded by ePSF and eI; therefore, the retrieved object information is closer to the original information. Figure 1 illustrates this physical concept.

3 Proof of Concept

The ME is the first order of the correlation function when the estimated transport mean free path within the scattering medium is substantially larger than the wavelength and is defined as[18,20]

$$C(qL) = [qL/\sinh(qL)]^2, \quad (4)$$

where L is the thickness of the scattering medium, $q = 2\pi\theta/\lambda$, θ is the scattering angle of the incident light, and λ is the incident wavelength. The ME can then be determined according to the full width at half-maximum of the correlation curve. To prove the concept of scattering state traversal, we devised an experiment to investigate a thin scattering medium. As shown in Fig. 2(a), a physical pinhole ($\emptyset = 200 \ \mu\text{m}$) illuminated by an incoherent light source (528 ± 10 nm, Daheng Optics GCI-060403) was placed on the optical axis of the imaging system. The diffractive light was projected onto a standard scattering
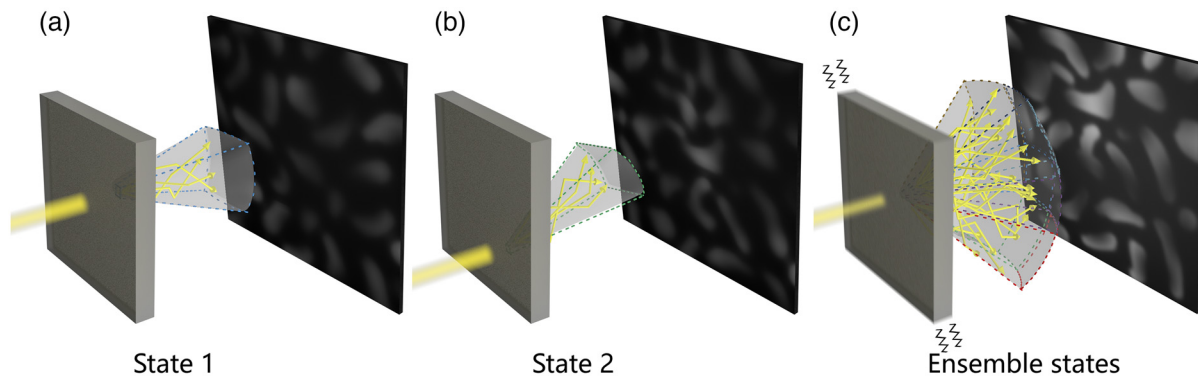
Fig. 1 Conceptual illustration of scattering state traversal. (a) A scattering state corresponds to a portion of the spatial information. The reconstruction range of the state is restricted by the ME range. (b) Another scattering state and (c) ensemble scattering states that traverse different scattering regions, enabling the retrieval of information beyond the ME range.

medium (Newport 5-deg circular light shaping diffuser) and diffused. The object plane was set at a distance of $d_o = 10$ mm from the diffuser.

In this experiment, the diffuser was suspended and swung as a pendulum. The string was $l = 300$ mm long, and the mechanical frequency was 0.91 Hz according to a simple calculation. It is worth noting that the mechanical frequency was intentionally set at a low value to ensure that the captured images were blurred. A higher frequency may weaken the diffusion property, leading to a scenario in which the "scattering photon" no longer dominates.[39] A monochromatic CMOS (Basler acA2040-90um) equipped with a main lens (Zeiss Milvus 2/100M ZF.2) was used to capture a series of similar PSF_ns at a shutter speed of 24 fps by placing a pinhole in the object plane. Then the pinhole was replaced by a 1.5-mm-long letter "G" as an object, and a series of images (I_ns) were captured at the same speed. The letter was hollow, while the outside was completely opaque.

Figures 2(b) and 2(c) show the ePSF and eI at different superposition times N. Because the PSF_ns and I_ns are captured at different times, the object cannot be reconstructed for $N = 1$, as shown in the first image in Fig. 2(d). However, as the number of superpositions increases, the reconstructed object becomes clearer, and the object is well distinguished when the number of superpositions reaches $N = 500$, as shown in the last image in Fig. 2(d). This finding demonstrates that the ePSF is effective for reconstructing unknown objects through time-variant scattering media. It is worth noting that the ballistic light is not significant when the number of superpositions exceeds 500, demonstrating that the target light is sufficiently scattered and recovered by the scattered light in a dominant manner.

4 Imaging Through Thick Turbid Media

According to Eq. (4), the ME range becomes narrower as the scattering medium becomes thicker. For example, when a typical static 1-cm-thick scattering medium is illuminated by incident light with $\lambda = 532$ nm, the ME angle is in the range of 0.1 mrad,[38,40] resulting in an extremely narrow ME range for practical applications. To prove that our proposed method can retrieve targets outside the ME range in thick scattering

media, the thin diffuser is replaced by a 1-cm-thick cuvette (inner dimension) containing a $CaCO_3$ turbid suspension.

The optical attenuation length can effectively characterize the scattering property of the media, and it can be obtained by measuring the transmittance of ballistic light.[17] As the demonstration experiments use a 528-nm LED, a laser light source with similar wavelength (532 nm) is used for the measurement. An optical power detector (Newport 818-ST2/DB) is used to measure the output light intensity with and without the $CaCO_3$ turbid suspension. A $\varnothing = 1$ mm iris was used to screen the ballistic light during the measurement. According to the measurement, the optical attenuation length of the suspension for the following experiment reaches 13.3, corresponding to a transport mean free path $l^* = 0.75$ mm.

The experimental setup is shown in Fig. 3(a). The object plane was set at a distance of $d_o = 12$ cm from the right surface of the cuvette. The illumination was provided by the same LED and shaped by a $\varnothing = 100$ mm, $f = 200$ mm convex lens to generate a uniform and sufficiently large spot. Before the experiment, the cuvette was treated with an ultrasonic cleaner to remove any $CaCO_3$ particles attached to the surface to prevent the formation of a static scattering layer. To prevent precipitates of the particles and ensure that the scattering property changed over time, the liquid was slowly agitated with a dropper purge. To obtain individual single states (or ensembles of partial states), the state-to-state differences must be within the numerical precision limit of the system. Thus to obtain speckle data with high numerical precision, a pco.edge 4.2 sCMOS with a dynamic range of 37,500:1 was used to capture the images. A Thorlabs MVL7000 lens was used to collect scattered light.

The reconstruction range of the scattering system is measured by calculating the normalized intensity of the recovered image when translating a round hole in the horizontal direction.[19,26,38] The same procedure is followed to evaluate the reconstruction range that can be achieved by our recovery method. The irradiance of an optical system decreases as the off-axis angle increases;[41] accordingly, the yellow curve in Fig. 3(b) shows this vignetting characteristic in the experimental setup, and the whole reconstruction range is measured to be ±205 mrad. Then a thick turbid medium is introduced, and the round hole image is reconstructed at various angles by

our proposed method (the number of superpositions is 1000). The blue dots in Fig. 3(b) illustrate the normalized intensity of each reconstructed image.

Figure 3(e) demonstrates that our method can consistently reconstruct images at different angles. The reconstruction range is close to the range of the original scattering system, indicating that the ePSF is effective for addressing ME limitations. The scattered results in Figs. 2 and 3 indicate that the experimental system experienced strong scattering, as the characteristics of

our results are significantly different from those of the ballistic light-based imaging process.

To directly visualize the reconstruction range beyond the ME range and evaluate the effect of our method with different objects, a series of letters are simultaneously placed in the object plane. The speckles in the image plane are captured with the above procedure. The letters and their reconstructed images are illustrated in Fig. 4, demonstrating the powerful ability of the ePSF to image beyond the ME range. According to Fig. 4(b),
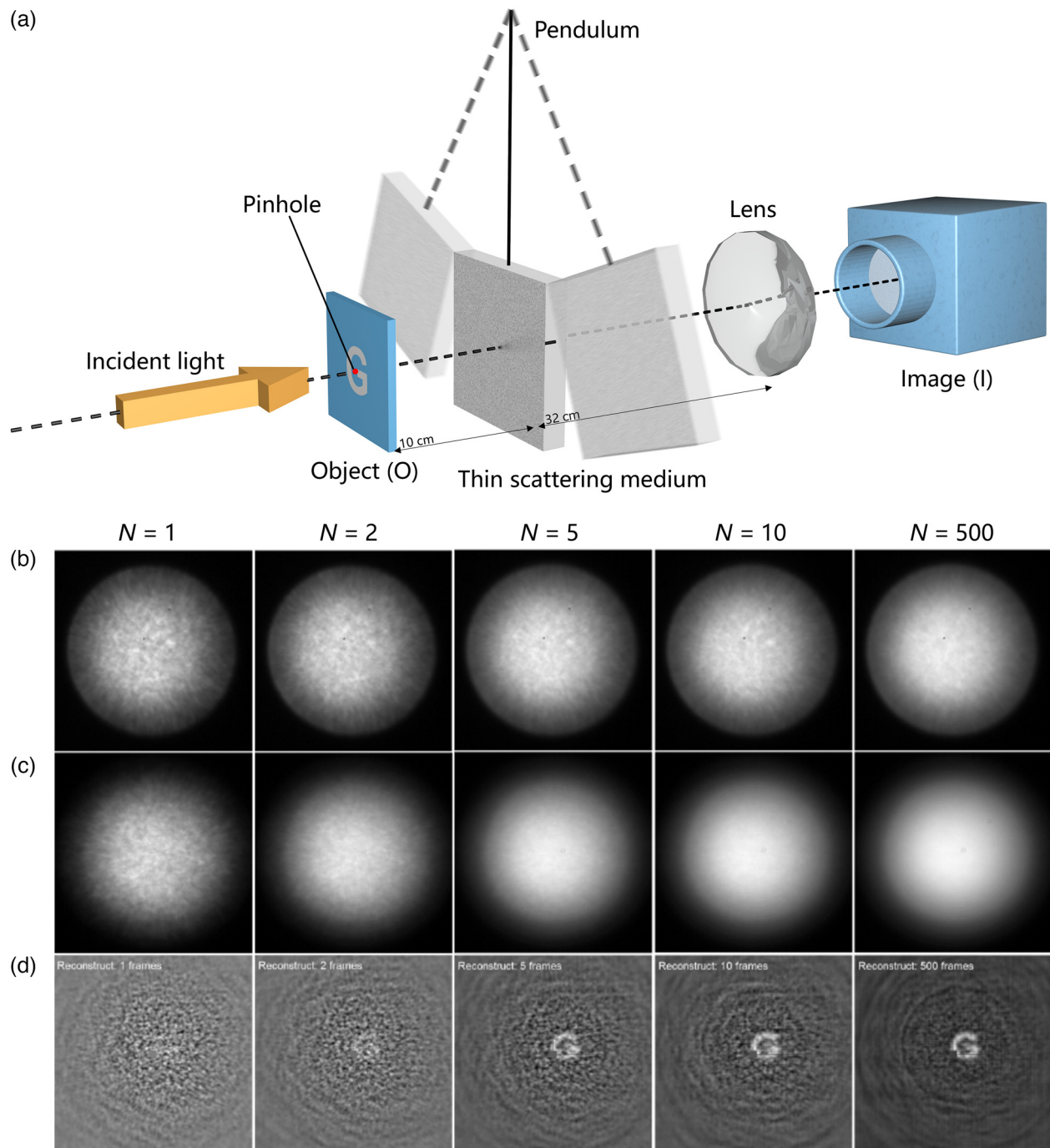
Fig. 2 Imaging through a dynamic diffuser approaching ergodicity. (a) Schematic of the experimental setup. The thin scattering medium swings as a pendulum. (b) ePSF, (c) eI, and (d) the reconstructed object at different superposition times N.
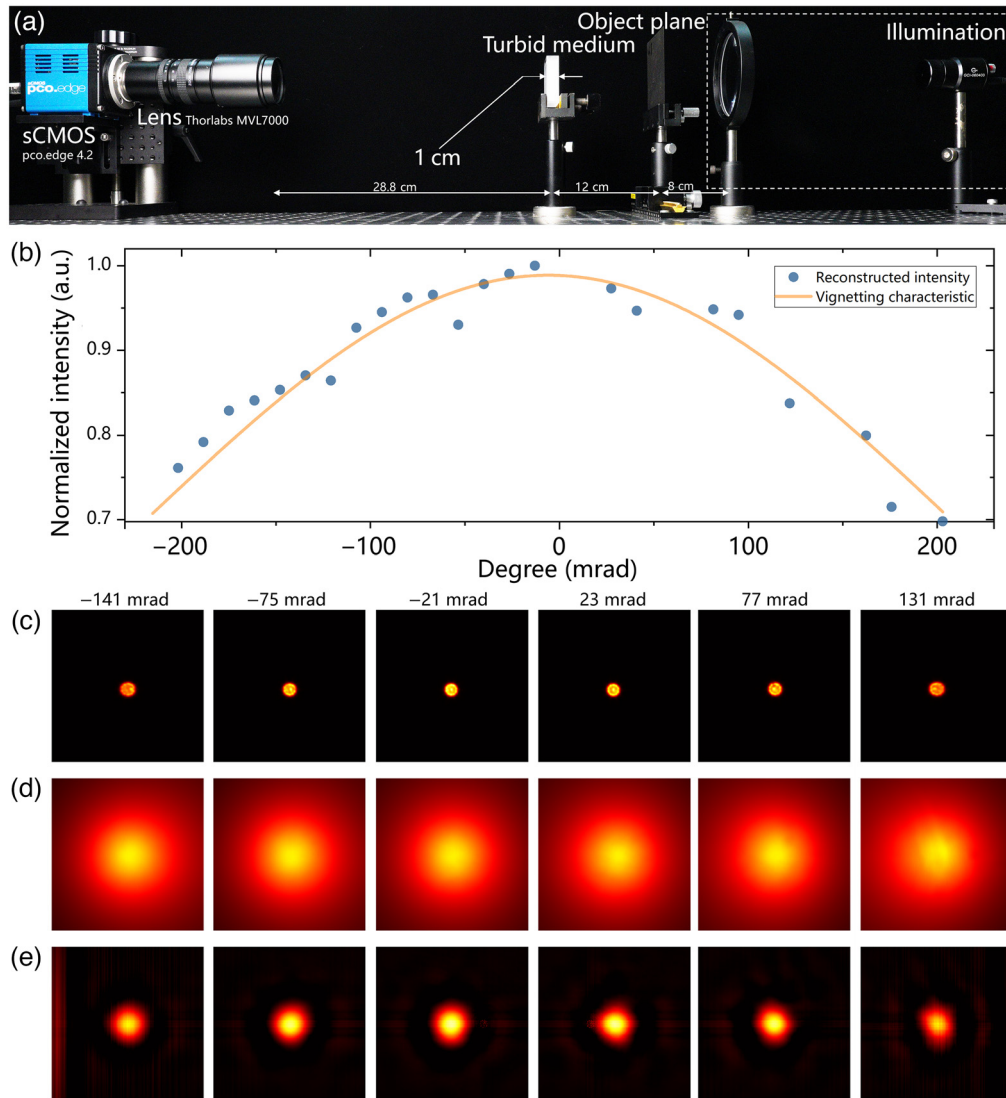
Fig. 3 Image reconstruction through a dynamic medium. (a) Experimental setup for the time-variant thick turbid medium. (b) Reconstructed intensity at different horizontal positions, showing the vignetting characteristic curve of our experimental setup. (c) Original, (d) scattered, and (e) reconstructed images of the round hole at various angles.

as the number of superpositions increases, the traversal of the scattering state is gradually completed. eI and ePSF both achieve ergodic scattering processes in a specific medium, consistently allowing the scattered target to be revealed at different positions in the reconstruction range. The quality of the reconstructed image is degraded compared to the raw image due to the aberrations from the imaging system and the signal-to-noise ratio of the speckle.

5 Discussion

It is worth noting that an ensemble of speckles is necessary for achieving ergodicity in reconstructed images in thick turbid media. Theoretically, each scattering state can be collected separately to determine the ensemble average. When the motion of a thin scatterer is regarded as a quasistatic process, the correlations among the speckles decrease with each small movement d, satisfying $d > r_{ME}$ (r_{ME} corresponds to the radius of the ME range, which is the same for every possible state, and d is described by the shifting velocity v and characteristic time τ as $d = v\tau$). The extraction of the speckles in each state requires fine control over the movement speed and exposure parameters. With specific coordination, it is possible to achieve image reconstruction for each state.[42,43] Moreover, shifting the diffusive media is an effective method for destroying the speckle structure and suppressing speckles.[44–46] For time-variant thick turbid media, the state changes caused by the overall macroscopic movement are transformed into various state changes caused by countless microscopic movements. Since the decorrelation time, which measures the state transition speed, is typically much smaller than the exposure time (from 10 to 200 ms in our experiments),[47] a single image contains an ensemble of multiple speckles in various states. A single image of speckles with a sufficiently long exposure time is theoretically equivalent to an ensemble of speckles after a series of images acquired over the same number of states. Both methods allow us to capture

(a)

(b)

$N = 50$

$N = 200$

$N = 500$

$N = 1000$

−205   −154   −102   −51   0   51   102   154   205 mrad
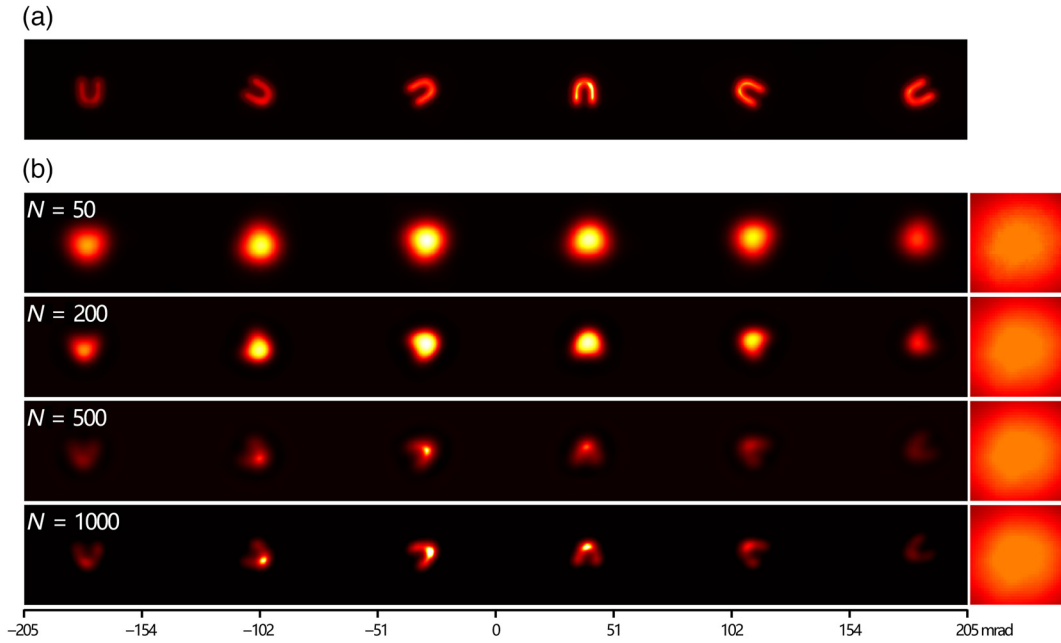
Fig. 4 Full range simultaneous reconstruction. (a) Raw object and (b) reconstructed object and the corresponding ePSFs at different superposition times N.

information about a large number of scattering states. However, imaging sensors cannot usually achieve a enough long exposure time due to insufficient dynamic ranges, leading to overexposure and a failure to reconstruct the target through thick turbid media, while an ensemble of speckles is effective at preserving as much scattering information about the object as possible. In addition, the proposed ergodic method is only applicable to the systems that are closed within the acquisition time. In the closed systems, the total ergodic states are finite, and the exact same sequence of PSFs can be traversed for several times to be matched with the measurement. However, for the open systems where the total ergodic states are infinite, the same sequence of scattering states cannot be traversed for another time, resulting in the failure of using the proposed method.

In practical application scenarios, objects originally existing in the background are usually known, such as bones, blood vessels, or fluorescent structures. Imaging targets are often emerging objects around known objects, such as abnormal biological tissue structures. The known objects O_R and the emerging targets O_T could form their corresponding ensemble speckle patterns eI_R and eI_T through the scattering media after reaching ergodicity:

$$\begin{cases} eI_R(x_i, y_i) = \int ePSF(x_i, y_i; x_o, y_o)O_R(x_o, y_o)dx_o\, dy_o \\ eI_T(x_i, y_i) = \int ePSF(x_i, y_i; x_o, y_o)O_T(x_o, y_o)dx_o\, dy_o \end{cases}. \quad (5)$$

As the convolution in the spatial domain is a multiplication in the spatial frequency domain, imaging targets can be recovered by the processing of the Fourier transform:

$$O_T = F^{-1}\left\{\frac{F\{eI_T\} \times F\{O_R\}}{F\{eI_R\}}\right\}, \quad (6)$$

where "F" represents the Fourier transform, and $\times$ indicates multiplication. Therefore, the *a priori* information can be used to image unknown targets over a large area.[48]

Using the same experimental setup in Fig. 3(a), as shown in Fig. 5, we know the letter "H" as a prior information. After the collection of its ensemble speckle, two unknown letters are
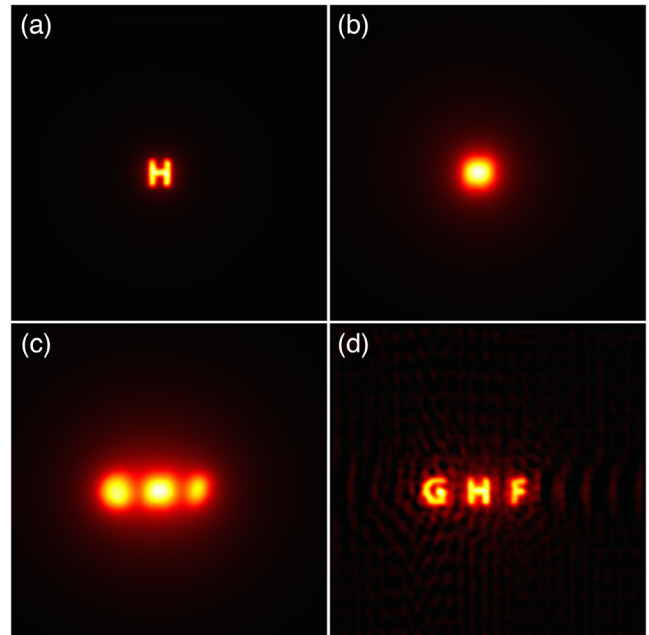
Fig. 5 Reconstruction of unknown targets with prior information. (a) Reference object, a letter "H," (b) ensemble speckle of the reference object, (c) ensemble speckle of the reference and unknown objects, and (d) reconstruction of the unknown objects, the letter "G" and "F."

inserted and form their corresponding ensemble speckles. With the process proposed in Eqs. (5) and (6), the unknown letters can be reconstructed to be "G" and "F."

6 Conclusions

We demonstrate that the PSF concept can be modified and extended to image through thick turbid media as long as the media are time variant. In this paper, the change in scattering media over time is used to reach ergodicity and obtain the ePSF, which allows the reconstruction range to exceed ME limits. The concept of the ePSF was developed to explain scattering state traversal and is capable of retrieving objects beyond the ME range in time-variant thick turbid media. We successfully applied this approach in experiments to reconstruct objects through a 1-cm-thick container filled with a stirring turbid liquid dispersion of $CaCO_3$ particles at visible incident wavelengths. The reconstruction range reaches the spatial limit of the scattering system and exceeds the ME range. Compared with static scattering media, time-variant scattering media exhibit temporal and spatial advantages in image recovery. We believe that this approach has great potential in various applications, such as biomedical imaging under strong diffusive circumstances.

Code, Data, and Materials Availability

The datasets used and analyzed during the current study are available from the corresponding author on reasonable request.

References

1. M. B. Nasr et al., "Demonstration of dispersion-canceled quantum-optical coherence tomography," *Phys. Rev. Lett.* **91**, 083601 (2003).
2. D. Debarre et al., "Image-based adaptive optics for two-photon microscopy," *Opt. Lett.* **34**, 2495–2497 (2009).
3. H. Kogelnik and K. S. Pennington, "Holographic imaging through a random medium," *J. Opt. Soc. Am.* **58**, 273–274 (1968).
4. I. M. Vellekoop and A. P. Mosk, "Focusing coherent light through opaque strongly scattering media," *Opt. Lett.* **32**, 2309–2311 (2007).
5. A. P. Mosk et al., "Controlling waves in space and time for imaging and focusing in complex media," *Nat. Photonics* **6**, 283–292 (2012).
6. H. Li et al., "Adaptive optical focusing through perturbed scattering media with a dynamic mutation algorithm," *Photonics Res.* **9**, 202–212 (2021).
7. Y. Luo et al., "Towards smart optical focusing: deep learning-empowered dynamic wavefront shaping through nonstationary scattering media," *Photonics Res.* **9**, B262–B278 (2021).
8. Z. Yu et al., "Wavefront shaping: a versatile tool to conquer multiple scattering in multidisciplinary fields," *Innovation* **3**, 100292 (2022).
9. P. Lai et al., "Photoacoustically guided wavefront shaping for enhanced optical focusing in scattering media," *Nat. Photonics* **9**, 126–132 (2015).
10. J. Schneider and C. M. Aegerter, "Guide star based deconvolution for imaging behind turbid media," *J. Eur. Opt. Soc. Rapid Publ.* **14**, 21 (2018).
11. H. He, Y. Guan, and J. Zhou, "Image restoration through thin turbid layers by correlation with a known object," *Opt. Express* **21**, 12539–12545 (2013).
12. W. Yang, G. Li, and G. Situ, "Imaging through scattering media with the auxiliary of a known reference object," *Sci. Rep.* **8**, 9614 (2018).
13. A. Boniface, J. Dong, and S. Gigan, "Non-invasive focusing and imaging in scattering media with a fluorescence-based transmission matrix," *Nat. Commun.* **11**, 6154 (2020).
14. L. Zhu et al., "Large field-of-view non-invasive imaging through scattering layers using fluctuating random illumination," *Nat. Commun.* **13**, 1447 (2022).
15. P. L. Hong, "Two-photon imaging assisted by a thin dynamic scattering layer," *Appl. Phys. Lett.* **113**, 101109 (2018).
16. Y. Sun et al., "Image reconstruction through dynamic scattering media based on deep learning," *Opt. Express* **27**, 16032–16046 (2019).
17. S. S. Zheng et al., "Incoherent imaging through highly nonstatic and optically thick turbid media based on neural network," *Photonics Res.* **9**, B220–B228 (2021).
18. M. J. Stephen and G. Cwilich, "Intensity correlation functions and fluctuations in light scattered from a random medium," *Phys. Rev. Lett.* **59**, 285–287 (1987).
19. S. Feng et al., "Correlations and fluctuations of coherent wave transmission through disordered media," *Phys. Rev. Lett.* **61**, 834–837 (1988).
20. I. I. Freund, M. Rosenbluh, and S. Feng, "Memory effects in propagation of optical waves through disordered media," *Phys. Rev. Lett.* **61**, 2328–2331 (1988).
21. J. Bertolotti et al., "Non-invasive imaging through opaque scattering layers," *Nature* **491**, 232–234 (2012).
22. O. Katz et al., "Non-invasive single-shot imaging through scattering layers and around corners via speckle correlations," *Nat. Photonics* **8**, 784–790 (2014).
23. W. Li et al., "Single-shot imaging through scattering media under strong ambient light interference," *Opt. Lett.* **46**, 4538–4541 (2021).
24. H. L. Liu et al., "Alternative interpretation of speckle autocorrelation imaging through scattering media," *Photonic Sens.* **12**, 220308 (2022).
25. E. Edrei and G. Scarcelli, "Optical imaging through dynamic turbid media using the Fourier-domain shower-curtain effect," *Optica* **3**, 71–74 (2016).
26. H. Zhuang et al., "High speed color imaging through scattering media with a large field of view," *Sci. Rep.* **6**, 32696 (2016).
27. X. Xie et al., "Extended depth-resolved imaging through a thin scattering medium with PSF manipulation," *Sci. Rep.* **8**, 4585 (2018).
28. J. P. Xie et al., "Depth detection capability and ultra-large depth of field in imaging through a thin scattering layer," *J. Opt.* **21**, 085606 (2019).
29. N. Antipa et al., "DiffuserCam: lensless single-exposure 3D imaging," *Optica* **5**, 1–9 (2018).
30. J. Rosen and D. Abookasis, "Noninvasive optical imaging by speckle ensemble," *Opt. Lett.* **29**, 253–255 (2004).
31. N. T. Shaked, Y. Yitzhaky, and J. Rosen, "Incoherent holographic imaging through thin turbulent media," *Opt. Commun.* **282**, 1546–1550 (2009).
32. D. Tang et al., "Single-shot large field of view imaging with scattering media by spatial demultiplexing," *Appl. Opt.* **57**, 7533–7538 (2018).
33. M. Chen et al., "Expansion of the FOV in speckle autocorrelation imaging by spatial filtering," *Opt. Lett.* **44**, 5997–6000 (2019).

34. X. Wang et al., "Prior-information-free single-shot scattering imaging beyond the memory effect," *Opt. Lett.* **44**, 1423–1426 (2019).
35. C. F. Guo et al., "Imaging through scattering layers exceeding memory effect range by exploiting prior information," *Opt. Commun.* **434**, 203–208 (2019).
36. I. Freund, "Looking through walls and around corners," *Phys. A: Stat. Mech. Appl.* **168**, 49–65 (1990).
37. X. Gan and M. Gu, "Effective point-spread function for fast image modeling and processing in microscopic imaging through turbid media," *Opt. Lett.* **24**, 741–743 (1999).
38. H. L. Liu et al., "Physical picture of the optical memory effect," *Photonics Res.* **7**, 1323–1330 (2019).
39. M. J. Purcell et al., "Holographic imaging through a scattering medium by diffuser-aided statistical averaging," *J. Opt. Soc. Am. Opt. Image Sci. Vis.* **33**, 1291–1297 (2016).
40. G. Osnabrugge et al., "Generalized optical memory effect," *Optica* **4**, 886–892 (2017).
41. Y. Q. Ji et al., "Non-uniformity correction of wide field of view imaging system," *Opt. Express* **30**, 22123–22134 (2022).
42. Y. Yuan and H. Chen, "Dynamic noninvasive imaging through turbid media under low signal-noise-ratio," *New J. Phys.* **22**, 093046 (2020).
43. T. F. Lu et al., "Non-invasive imaging through dynamic scattering layers via speckle correlations," *Opt. Rev.* **28**, 557–563 (2021).
44. S. Lowenthal and D. Joyeux, "Speckle removal by a slowly moving diffuser associated with a motionless diffuser," *J. Opt. Soc. Am.* **61**, 847–851 (1971).
45. Y. Kuratomi et al., "Speckle reduction mechanism in laser rear projection displays using a small moving diffuser," *J. Opt. Soc. Am. Opt. Image Sci. Vis.* **27**, 1812–1817 (2010).
46. S. Kubota and J. W. Goodman, "Very efficient speckle contrast reduction realized by moving diffuser device," *Appl. Opt.* **49**, 4385–4391 (2010).
47. M. M. Qureshi et al., "In vivo study of optical speckle decorrelation time across depths in the mouse brain," *Biomed. Opt. Express* **8**, 4855–4864 (2017).
48. X. Xu et al., "Imaging objects through scattering layers and around corners by retrieval of the scattered point spread function," *Opt. Express* **25**, 32829–32840 (2017).

Yuyang Shui received his BEng and MEng degrees from Sun Yat-Sen University in 2019 and 2021, respectively. He is currently a PhD candidate at the School of Physics of Sun Yat-Sen University. His research interests include scattering imaging, computational imaging, event-based vision, and intelligent vision.

Ting Wang received her BS degree from Hunan Normal University in 2021. She is currently a postgraduate student at the School of Physics and Astronomy of Sun Yat-sen University. Her research interests include scattering imaging, computational imaging, and event-based vision.

Jianying Zhou received his BS degree from Huazhong University of Science and Technology in 1982 and his PhD in optics from the Imperial College London, United Kingdom, in 1988. He was the director of the State Key Laboratory of Ultrafast Laser Spectroscopy at Sun Yat-sen University, from 1994 to 1999. He was the director of the School of Physics and Engineering at Sun Yat-sen University, from 1996 to 1999. He is currently a professor at the School of Physics of Sun Yat-sen University. His current research interests include ultrafast optoelectronics, optical imaging recovery, super-resolution optical imaging, and optics in virtual reality and in 3D display technology.

Xin Luo received his BS and PhD degrees from Sun Yat-sen University in 2006 and 2011, respectively. He is currently a professor at the School of Physics of Sun Yat-sen University. His current research interests include low-dimensional material and first principle calculation.

Yikun Liu received his BS and PhD degrees from Sun Yat-sen University in 2006 and 2013, respectively. He is an associate professor at the School of Physics and Astronomy of Sun Yat-sen University. His current research interests include optical imaging and nonlinear optics.

Haowen Liang received his BS and PhD degrees from Sun Yat-sen University in 2011 and 2016, respectively. He is an associate professor at the School of Physics of Sun Yat-sen University. His current research interests include metalense, scattering imaging, and virtual reality technology.